

SAND REPORT

SAND2001-3773
Unlimited Release
Printed December, 2001

Using the Saturn Accelerator for Isentropic Compression Experiments (ICE)

Michael D. Furnish, Jean-Paul Davis, Marcus Knudson, Tom Bergstresser,
Christopher Deeney, and James R. Asay

Prepared by
Sandia National Laboratories
Albuquerque New Mexico 87185 and Livermore, California, 94550

Sandia is a multiprogram laboratory operated by Sandia Corporation,
A Lockheed Martin company, for the United States Department of
Energy under Contract DE-AC04-94AL85000

Approved for public release; further dissemination is unlimited.



Sandia National Laboratories

Issued by Sandia National Laboratories, operated for the United States Department of Energy by Sandia Corporation.

NOTICE: This report was prepared as an account of work sponsored by an agency of the United States Government. Neither the United States Government, nor any agency thereof, nor any of their employees, nor any of their contractors, subcontractors, or their employees, make any warranty, express or implied, or assume any legal liability or responsibility for the accuracy, completeness, or usefulness of any information, apparatus, product, or process disclosed, or represent that its use would not infringe privately owned rights. Reference herein to any specific commercial product, process, or service by trade name, trademark, manufacturer, or otherwise, does not necessarily constitute or imply its endorsement, recommendation, or favoring by the United States Government, any agency thereof, or any of their contractors or subcontractors. The views and opinions expressed herein do not necessarily state or reflect those of the United States Government, any agency thereof, or any of their contractors.

Printed in the United States of America. This report has been reproduced directly from the best available copy.

Available to DOE and DOE contractors from
U.S. Department of Energy
Office of Scientific and Technical Information
P.O. Box 62
Oak Ridge, TN 37831

Telephone: (865)576-8401
Facsimile: (865)576-5728
E-Mail: reports@adonis.osti.gov
Online ordering: <http://www.doe.gov/bridge>

Available to the public from
U.S. Department of Commerce
National Technical Information Service
5285 Port Royal Rd
Springfield, VA 22161

Telephone: (800)553-6847
Facsimile: (703)605-6900
E-Mail: orders@ntis.fedworld.gov
Online order: <http://www.ntis.gov/ordering.htm>



Using the Saturn Accelerator for Isentropic Compression Experiments (ICE)

Michael D. Furnish¹, Jean-Paul Davis², Marcus Knudson², Tom Bergstresser¹, Christopher Deeney¹, and James R. Asay²

¹Energetic Experiments & System Instrumentation Department

²Weapon Science Applications Department

Sandia National Laboratories

Albuquerque NM 87185-1168

Abstract

Recently an innovative technique known as the Isentropic Compression Experiment (ICE) was developed that allows the dynamic compressibility curve of a material to be measured in a single experiment. Hence, ICE significantly reduces the cost and time required for generating and validating theoretical models of dynamic material response. ICE has been successfully demonstrated on several materials using the 20 MA Z accelerator, resulting in a large demand for its use. The present project has demonstrated its use on another accelerator, Saturn. In the course of this study, Saturn was tailored to produce a satisfactory drive time structure, and instrumented to produce velocity data. Pressure limits are observed to be approximately 10-15 GPa ("LP" configuration) or 40-50 GPa ("HP" configuration), depending on sample material. Drive reproducibility (panel to panel within a shot and between shots) is adequate for useful experimentation, but alignment fixturing problems make it difficult to achieve the same precision as is possible at Z. Other highlights included the useful comparison of slightly different PZT and ALOX compositions (neutron generator materials), temperature measurement using optical pyrometry, and the development of a new technique for preheating samples. 28 ICE tests have been conducted at Saturn to date, including the experiments described herein.

Acknowledgments

We gratefully acknowledge the assistance and cooperation of the Saturn staff, especially Brad Peyton and Matt Torres. The VISARs and recorders were configured and operated by Ed Marsh, Greg Mize, Dennis Barker, and Steve Becker of Bechtel Nevada, assisted in later shots by Scott Walker and Richard Hacking. Chris Russell (“Lab 101”) performed the detailed design work for the experiment hardware and deserves much thanks for his patience and careful work. Major portions of the basic panel design for ICE are due to Clint Hall, whom we thank. Dave Reisman of LLNL assisted with deriving the pressure/volume path for Shot 2901.

This work was performed under the LDRD program at Sandia National Laboratories (Project 32576) , supported by the U. S. Department of Energy under contract DE-AC04-94AL85000. Sandia is a multiprogram laboratory operated by Sandia Corporation, a Lockheed Martin company, for the USDOE.

Table of Contents

1.0	Introduction and Motivation.....	7
2.0	Feasibility study: Initial 6 experiments.....	9
2.1	Focus of this effort	9
2.2	Facility modifications and diagnostics.....	9
2.3	Experiments	10
2.4	Results.....	12
2.5	Assessment.....	16
3.0	Other configurations, validations and diagnostics.....	17
3.1	Single-sided slab drive concept.....	17
3.2	Ferroelectric and encapsulant comparison shots with containment extension.....	19
3.3	Pre-molten tin: Resistively heated samples	21
3.4	IR interferometry.....	22
3.5	Other configurations and notes.....	24
4.0	Overall summary.....	25
	Appendix A: Additional drawings of experiment hardware.....	26
	Appendix B: Effects of various Saturn transmission line elements on pulse timing...	28
	References	30
	Distribution	31

Figures

1.1	Schematic of operation of isentropic compression method.....	7
1.2	Saturn ICE configuration (Top) Perspective; (Bottom) Schematic.....	8
2.2.1.	Predicted velocity histories for Saturn 2494	10
2.4.1	Results from Test 2900 (LP configuration, LP machine mode).....	12
2.4.2	Results from Test 2901 (LP configuration, LP machine mode).....	13
2.4.3	Results from Test 2902 (HP configuration, LP machine mode).....	14
2.4.4	Comparison of current input for Shots 2902, 2904 and 2906.....	15
2.4.5	Velocity histories for Shot 2904	15
2.4.6	Velocity histories for Shot 2906	16
3.1.1	Configuration of single-sided slab experiment	17
3.1.2	VISAR records from single-sided slab experiment	18
3.2.1	Configuration of PZT LP shots.....	19
3.2.2	Velocity results from PZT tests 2912, 2919	20
3.2.2	Velocity results from tests 2913 (ALOX)	20
3.3.1	Resistive-heating cell used to obtain pre-molten tin samples on Saturn.....	21
3.3.2	Example of velocity data obtained on Saturn for isentropic compression of molten tin at approximately 600K, showing a signature possibly due to dynamic freezing.	22
3.4.1	Left: Schematic of the Pyrometer. Right: Sketch of the Probe.....	23

3.4.2	Bottom: VISAR data from Saturn experiment 2915; Top: Apparent temperature from the same experiment.....	24
A.1	LP ICE configuration. (Top) Top view (Bottom) Side view.....	26
A.2	HP ICE configuration. (Top) Top view (Bottom) Side view	26
B.1.	Effects of circuit elements on downline pulses at Saturn (from Shot 2904).....	28

Tables

2.3.1	Initial set of tests.....	11
B.1	Line configurations for Saturn shots 2904, 2906.....	29

Using the Saturn Accelerator for Isentropic Compression Experiments (ICE)

1.0 Introduction and Motivation

With the recent demonstration of successful isentropic compression experiments at the Z accelerator [Asay, 1999; Hall, 2000; Hall et al, 2001; Reisman et al, 2001], increased interest from numerous laboratories has caused a demand for shots exceeding those available at Z. Inasmuch as a significant fraction of this demand is for experiments to peak stress levels lower than the 50 – 200 GPa available in magnetic drive experiments at Z, a logical next step is to begin performing ICE experiments on the lower-current Saturn accelerator. Z is a 20 MA machine, and Saturn is capable of driving approximately 10 MA into similarly inductive targets. Since the magnetic drive pressure is roughly proportional to the square of the current, Saturn is capable of driving a 10 – 50 GPa ramp load into a variety of samples.

The isentropic compression method in these accelerators capitalizes on the ramp pulse naturally produced. As the current propagates up a conductor termed the cathode, then returns via a panel (anode) mounted close to the cathode, the resulting $\mathbf{J} \times \mathbf{B}$ magnetic forces act to accelerate the panel away from the cathode. With the ramp structure (100 – 200 ns rise), this drives a ramp pressure pulse of similar rise time into samples mounted to the panel surface. Measuring the velocity histories of the rear surfaces of two or more samples of different thicknesses of a test material under these conditions provides sufficient information for deducing the continuous compressibility curve for the sample material. If the material exhibits rate dependence, a measurement of the velocity of the surface of the panel is also needed to provide enough data to deduce the material properties of the sample. This is illustrated in Fig. 1.1.

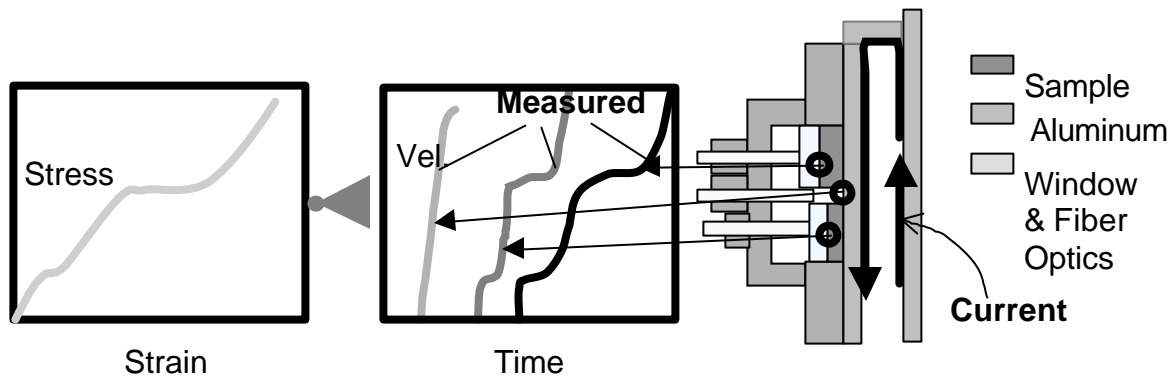


Figure 1.1. Schematic of operation of isentropic compression method.

The basic design of the ICE configuration required for Saturn, which may be described as an upside-down Z configuration, is shown in Fig. 1.2. This structure is placed at the bottom of the MITL stack in the Saturn center section, with fiber-optic-coupled diagnostics (VISAR or pyrometry) positioned by the caps over the samples. Key to the proper functioning of the experiment is whether the gaps between the cathode and the anode plates can be accurately prescribed and measured. Tolerances of 1 mil are needed for these gaps.

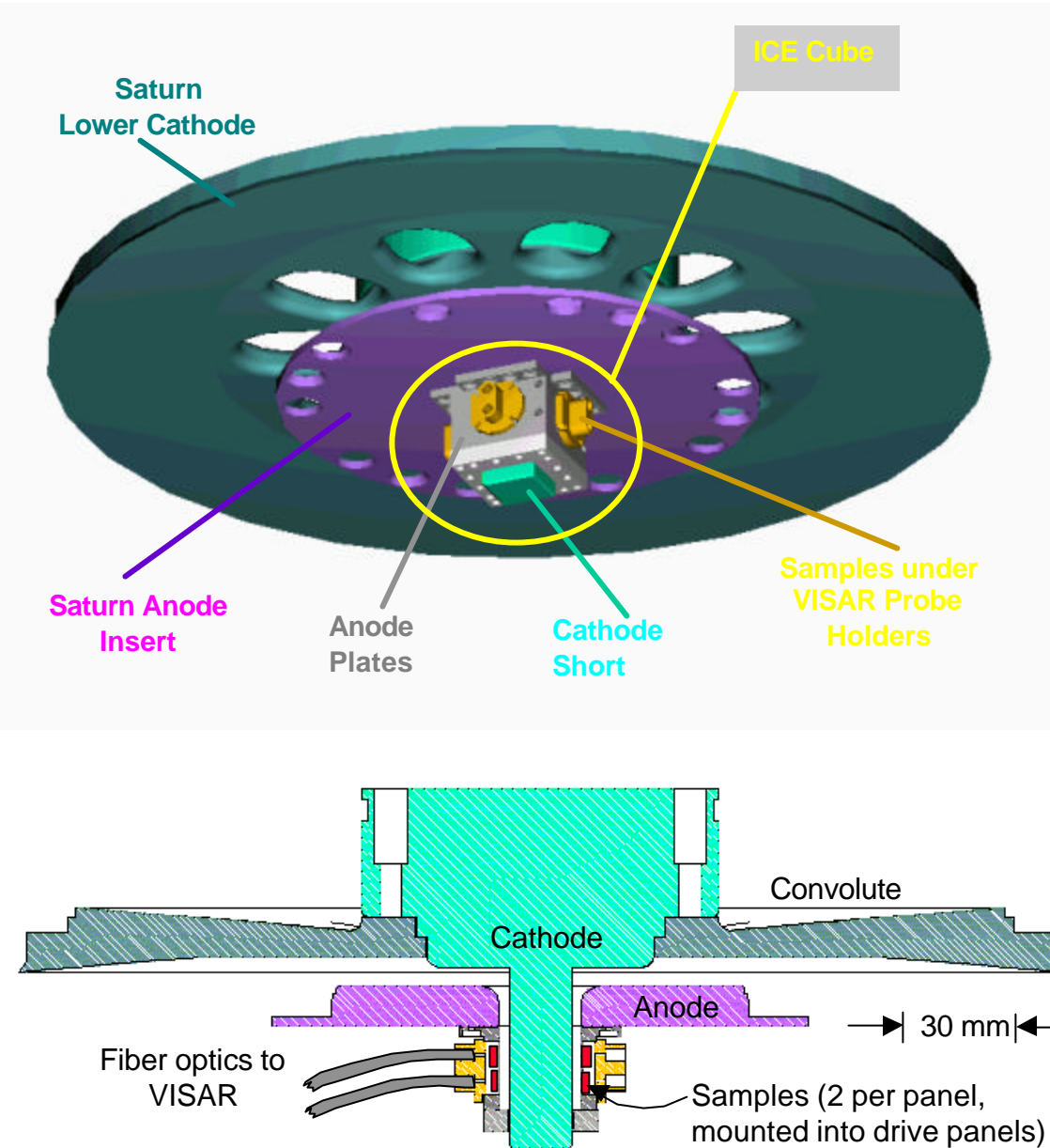


Figure 1.2. Saturn ICE configuration (Top) Perspective; (Bottom) Schematic.
Note: For many of the present experiments, the drive panels, i.e. the walls at the base of the counterbores, were used as samples)

2.0 Feasibility Study: Initial 6 Experiments

2.1 Focus of this effort

In ICE experiments in a production mode, samples are mounted on “drive panels” formed by machining counterbores in the anode panels. However, for the initial assessment of Saturn for ICE studies, we considered it preferable to use the drive panels themselves as “samples.” This eliminated the variables inherent with samples whose properties are not well known (for example, aluminum or copper), and allowed a better assessment of the method used in conjunction with this facility.

This assessment was aimed to determine whether:

- The ICE configurations demonstrated on Z could be translated to Saturn;
- The appropriate drive uniformity required for accurate EOS characterizations could be achieved, and
- 1 – 2 % accuracy is possible on Saturn.

2.2 Facility modifications and diagnostics

Prior to performing these experiments, three areas had to be addressed. First, the ICE design had to be adapted for Saturn. Changes required for the anode panels were quite minor due to the modularity of the system and similarity to Z. New convolutes had to be manufactured. A new assembly of MITLS (magnetically insulated transmission lines, which are upstream of the inserts shown in Fig. 1.2, had already been fabricated. Ideally, a new cathode convolute should be used for each shot to give accurate alignment.

Second, to allow the use of VISAR diagnostics, fiber optic harnesses were installed and a location for the instruments and lasers had to be determined and readied. The instruments were set up in the user screen room, together with the Verdi lasers. This required the manufacture and installation a 40-fiber harness of 200 micron fibers from the screen room to the outside of the vacuum feedthru in to the center section, and a second harness through the feedthru. All fiber ends were equipped with standard ST connectors. The fiber optic probes used, which in most cases are bare-fiber probes positioned 0.5 – 5 mm from the sample surface, are equipped with ST connectors to connect to the feedthru harness. The probes are the only portion of this system considered disposable. Finally, the signal transit times through the fibers were measured using a pulsed-laser system of the same wavelength as the supply light used for the VISARs (532 nm).

Finally, it was necessary to have a preliminary idea of how to configure the transmission line elements of Saturn to deliver the appropriate pulse structure to the ICE panels at the machine center, both for purposes of tailoring the waveform and designing the panels to appropriately use this waveform. Earlier experiments (Saturn shot 2478 and after) had produced a long risetime waveform (230 ns start to peak) into a short circuit load. On that experiment a ramp time of 230 ns was observed (current squared vs. time; imposed stress is proportional to current squared). Based on results from these experiments, representative model velocity histories were calculated for a range of thicknesses in aluminum drive panels; results are shown in Fig. 2.2.1.

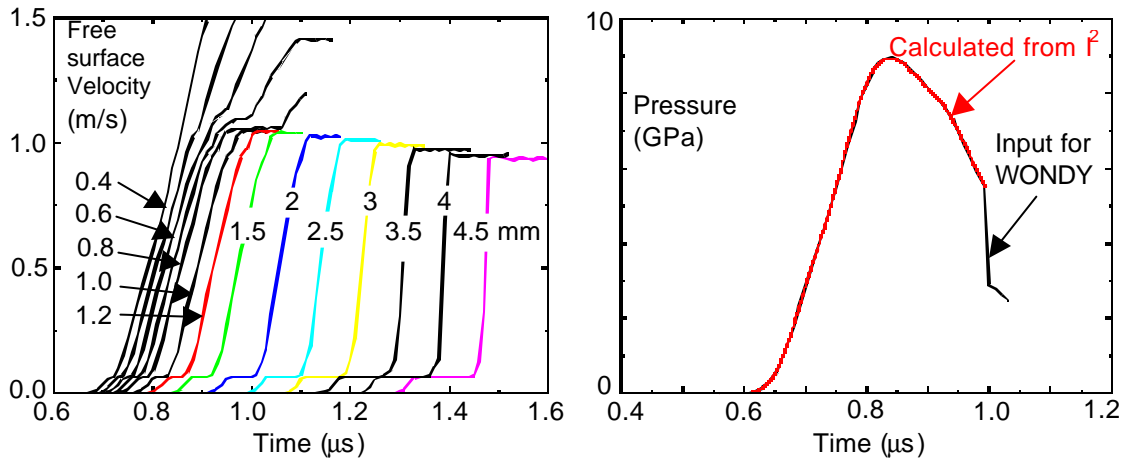


Figure 2.2.1. (Left) Predicted velocity histories for Saturn 2901 current history into an aluminum ICE panel. Thicknesses of the aluminum samples (drive panels) are shown. (Right) Drive profile derived from 2901 current history

The wave histories shown in Fig. 2.2.1 illustrate that certain limitations must be observed in the design of ICE experiments. In particular, the ramp time limits the thicknesses of the drive panels and the samples. The drive panel (the surface on which the sample is placed) must be thick enough that the complete ramp enters the sample before the reflection of the toe of the ramp back into the panel is able to re-reflect from the inside surface of the panel and reach the sample. If the panel is too thin, the later part of the rise is perturbed by the re-reflected toe of the ramp (Fig. 2.2.1 left: note behavior of 0.1 and 0.2 mm thick panels). A similar condition provides a minimum thickness for the sample when it is distinct from the drive panel. Maximum thicknesses are dictated by the need to avoid steepening of the ramp into a shock within the panel or the sample (Fig. 2.2.1 left: 2.0 mm thickness). Such steepening occurs for most materials.

2.3 Experiments

A matrix of experiments was designed as shown in Table 2.3.1. These experiments were aluminum¹ panel shots² with no windows. Diagnostics were VISAR interferometry on each sample (2 samples per panel, 4 panels per experiment). Dual-delay interferometry was used for 6 of the 8 samples, with single-delay for the remaining two samples. Dual delay means that the returned light from a sample was input to two VISARs with different sensitivities. Since 14 channels of VISAR were available for this study (2 7-beam systems), it was not possible to provide dual-delay for all 8 samples.

¹ Copper was originally planned, but aluminum was delivered and these were used.

² For the experiments of Section 2, the samples were the panel walls, counterbored to the thicknesses noted, with diamond-machined finishes. In later experiments, samples were mounted to the counterbore surface, with or without windows (fused silica, LiF or sapphire, attached to the sample, where the VISAR monitors the sample/window interface).

Two styles of panel / cathode configuration were used: LP (Low Pressure) and HP (High Pressure). The HP configuration utilizes an 11 mm square cathode, with a 2 mm gap between the cathode and the anode panels. The LP configuration is slightly larger and includes a 3 mm gap between the cathode and the anode panels. The smaller plan cross-section of the HP configuration gives a higher current density, hence a higher drive pressure. Each holds 8 samples. Detailed diagrams are included in Appendix A.

Table 2.3.1. Initial set of tests. Specifications were for Cu panels; Al was supplied.

Test #	Rise Time (μs)	Config [Ⓝ]	Pulse Mode*	N Top	N Bot	W Top	W Bot	S Top	S Bot	E Top	E Bot
2900	0.140	LP	LP	0.4	0.7	0.6	0.7	0.8	0.7	1.0	0.7
2901	0.280	LP	LP	1.0	1.2	1.5	1.2	2.0	1.2	2.5	1.2
2902	0.140	HP	LP	0.4	0.7	0.6	0.7	0.8	0.7	1.0	0.7
2904	0.140	HP	ELP	0.4	0.7	0.8	0.7	0.8	0.7	1.0	0.7
2906	0.280	HP	ELP	0.7	0.8	0.9	0.8	1.3	0.8	1.7	0.8
2903	0.140	HP, 1 mm	SP	0.4	0.7	0.6	0.7	0.8	0.7	1.0	0.7

*Pulse Mode: LP = “long pulse,” SP = “short pulse” (modified; prepulse gaps closed), ELP = extra-long pulse (same config. as Shot 2899)

[Ⓝ] Target Config: LP = low pressure 4-panel assembly, HP = high pressure 4-panel assembly

One strength of Saturn is that the current time profile may be adjusted line-by-line over the 36 lines available. Major components of the circuitry involved, which may be adjusted line-by-line, include:

- Cable length and additional delay cables from the pulse distribution system (the “spider”)
- Jumpers at the Marx generator output (15 ns delay)
- Sets of 5 breakdown pins for line pairs which may be shorted to advance the timing of the current pulse transmitted down a given line.
- A prepulse gap at the input to the pulse-forming (water) section which may be shorted or opened.

The principal difference between the SP and LP machine configurations lies in the shorting of the breakdown pins; when these are shorted a long pulse results, however, leaving them open delays the pulse until it is built sufficiently from Marx discharge to provide a very short ramp about 150 ns later in time.

A hybrid configuration, used for two of the later shots (2904, 2906), utilized a variety of combinations of pin shortings, prepulse gaps states, and jumpers to spread out the current arrival at the load. This was termed an “ELP” (extra-long pulse) configuration. Details are shown in Appendix B. Results were not completely satisfactory (see below), and the LP mode remains the best configuration for ICE work at Saturn. However, the possibility exists of finding a better combination in the future.

2.4 Results

The first three tests (2900 – 2902) were conducted using the long-pulse machine configuration. 2902 used the HP configuration; the other two used the LP configuration. Results¹ from 2900 are shown in Fig. 2.4.1. The maximum stress is estimated as 10 GPa.

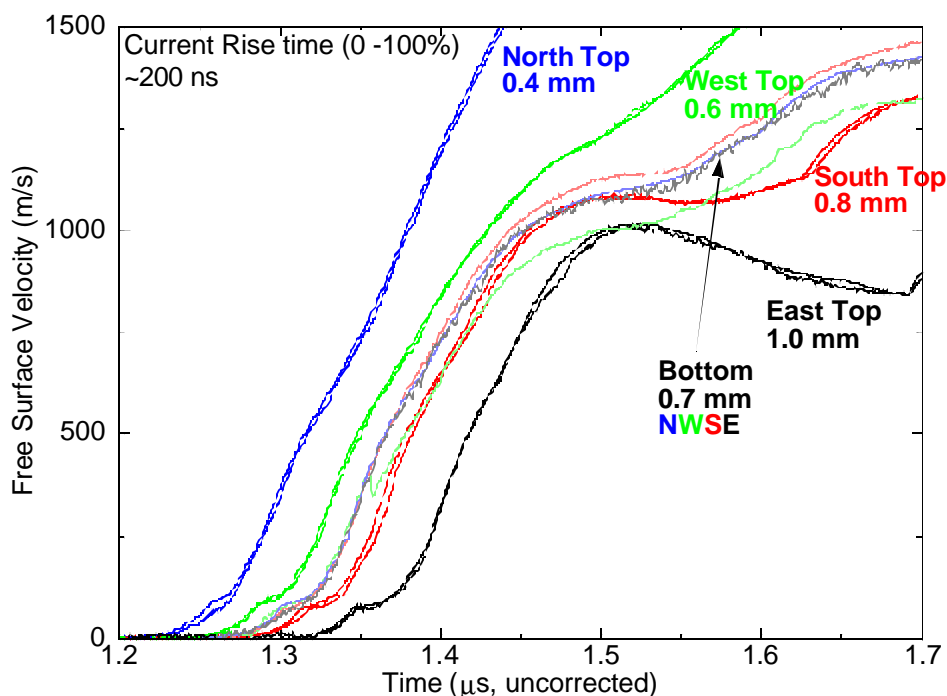


Figure 2.4.1. Results from Test 2900 (LP configuration, LP machine mode).

The elastic precursor is clearly present at the toe of the waves. Data quality appears good, as does panel-to-panel uniformity (evidenced by the consistency of the bottom samples).

Results from 2901 are shown in Fig. 2.4.2. This test utilized thicker drive panels. Shock-up is only beginning in the thickest panel (2.5 mm), consistent with the relatively low pressures involved for these tests. Timing for this test has been carefully established based on signal and timemark transit times and timemark readings on the digitizers. Again, the maximum stress is estimated as 10 GPa. The elastic precursor is clearly present at the toe of the waves. Again, data quality appears good, as does panel-to-panel uniformity. The current rise time was ~ 230 ns, typical of these LP shots.

Pressure-density data were derived from these velocity histories by a characteristics method, corrected for the refractive effect of the release ramp reflected from the free surface. Results are shown in Fig. 2.4.2 (lower left).

¹ A “cosine correction” is not included in these results. Such a correction is typically 1-2%, and arises because the light delivered to the sample by the supply fiber and reflected into the return fiber follows a path not completely normal to the sample surface. This applies to all results presented in the present report.

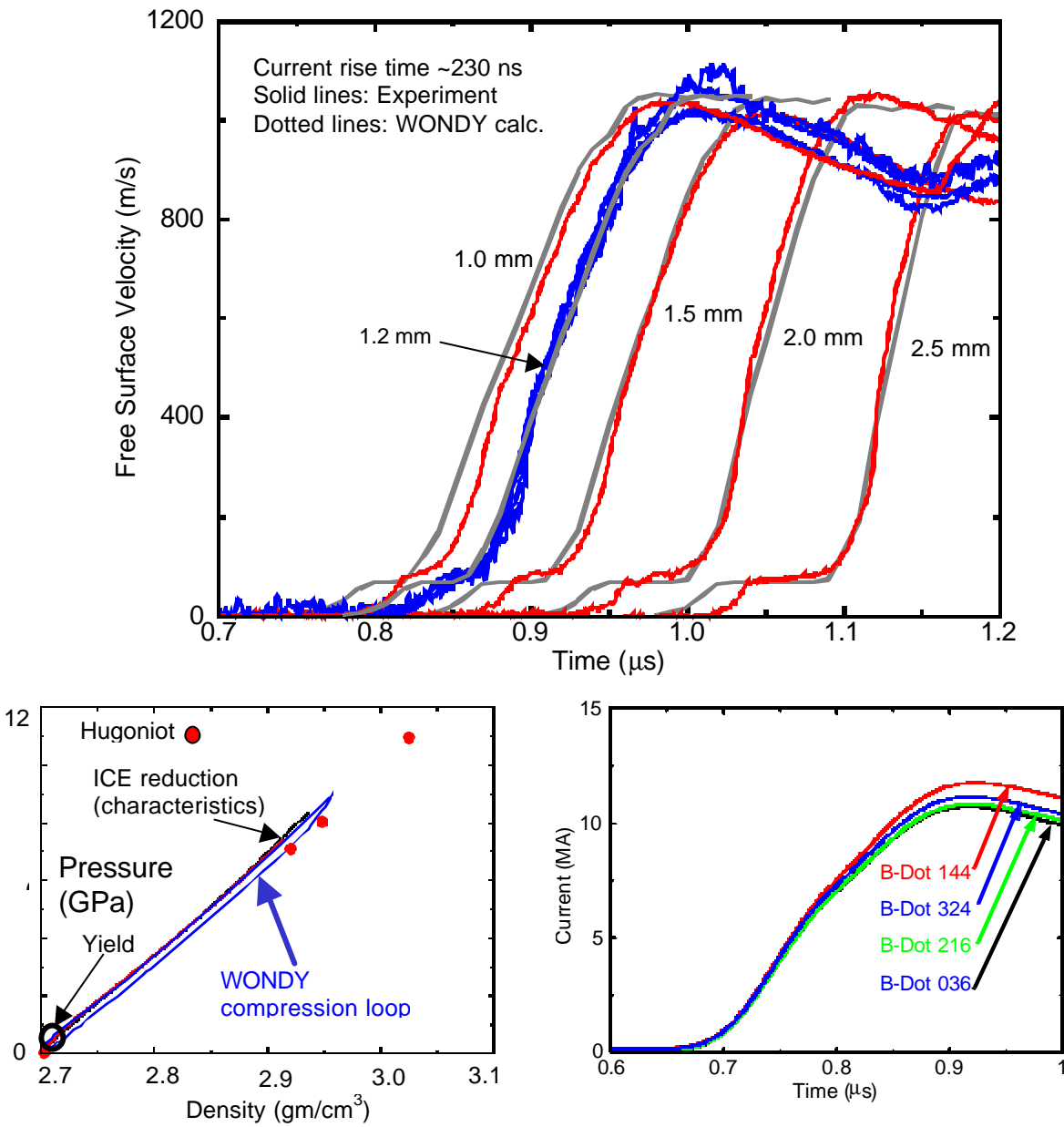


Figure 2.4.2. Results from Test 2901 (LP configuration, LP machine mode). Top: Velocity histories. Left: Derived pressure-density plot. Right: Current record (same timebase as velocity histories above).

Shot 2902 utilized the HP panel configuration and the LP machine mode. Results are shown in Fig. 2.4.3. Maximum stress produced is estimated as 40 GPa. This plot includes not only the initial arrivals (most useful for deriving isentropic compression curves), but subsequent panel behavior. As can be seen, the thinnest panels (north top and west top) do not show a clear break between the initial ramp arrival and arrival of the reflected reload pulse from the back of the panel. Hence these two drive panels are too thin for the ramp duration. This is consistent with the higher wavespeed in aluminum (used) than in copper (expected).

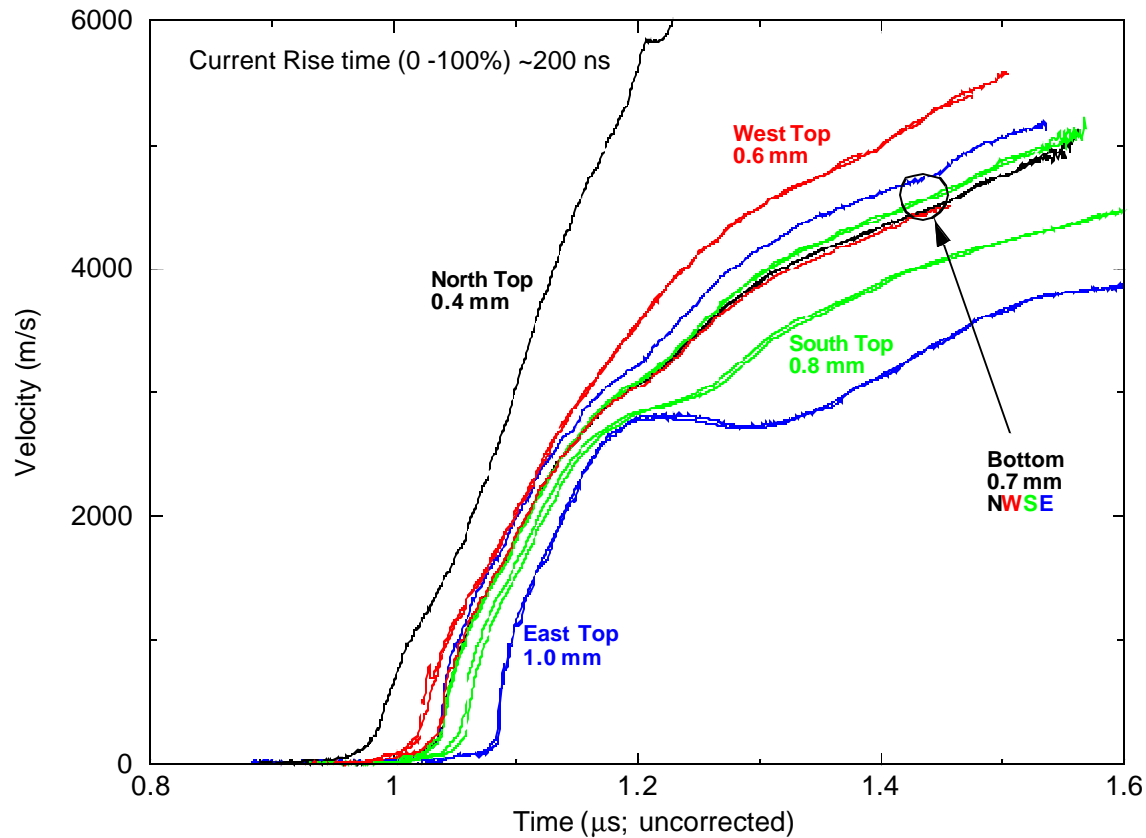


Figure 2.4.3. Results from Test 2902
(HP panel configuration, LP machine configuration)

Shot 2903 unsuccessfully utilized the SP Saturn machine mode. Noting that the Saturn LP machine mode with ICE experiments gave a longer rise time than without (Experiments 2900-2902: 200-230 ns, vs. 2594: 140 ns)¹, we scheduled a HP panel assembly to be used with a SP mode test for Shot 2903. Unfortunately the HP assembly used had a 1 mm anode-cathode gap (vs. 2 mm for 2902), so a lower inductance than in 2900-2902. The Saturn ramp produced was fast enough to band-edge the digitizers acquiring the b-dot information (time derivative of current). The loading time was approximately 70 ns.

Shots 2904 and 2906 were intended to repeat Shot 2902 (HP panel configuration, range of panel thicknesses) except for a longer rise-time machine configuration (“ELP”), which was discussed above (Section 2.3). The current input is shown in Fig. 2.4.4, stacked against the input from Shot 2902. Neither was a successful ICE experiment. For Shot 2904 (Fig. 2.4.5), most panels displayed a shock in the loading. From such profiles it is not possible to derive a continuous isentropic loading curve. In Shot 2906 (Fig. 2.4.6), the shock is more dominant. To be truly useful, this input wave structure needs to be more carefully tailored to give a better transition from the toe to the upper rise.

¹ Possibly a false interpretation; shot 2494 was a Z-pinch shot, which (as noted above) has an earlier cutoff than would ICE experiments.

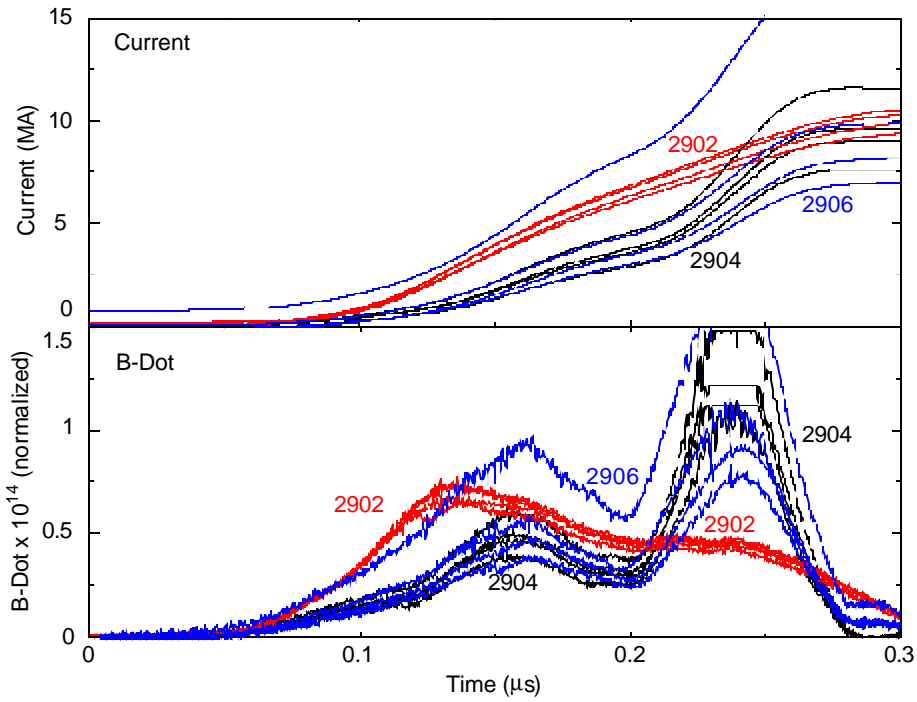


Figure 2.4.4 Comparison of current input for Shots 2902, 2904 and 2906.

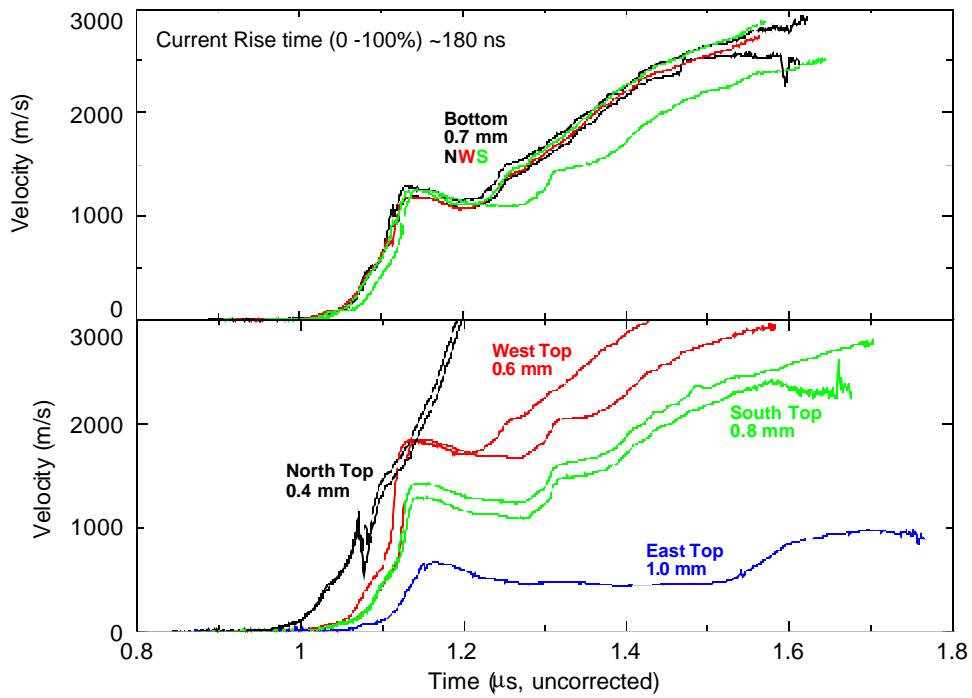


Figure 2.4.5. Velocity histories for Shot 2904. Timebase is not correlated with that of Fig. 2.4.4.

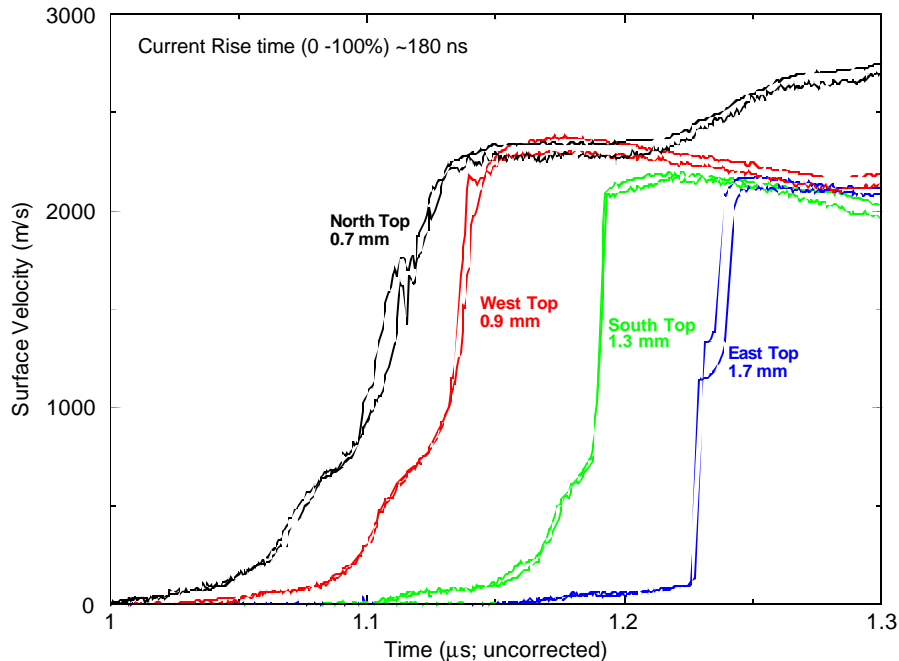


Figure 2.4.6. Velocity histories for Shot 2906.
Bottom panel measurements omitted for clarity.

2.5 Assessment

These shots represent a qualified success.

- The LP (long-pulse) machine configuration appears to provide a useful current structure for general-purpose ICE experiments
- The cost is significantly below that for Z; as well, time is far more available.
- The available pressure levels are useful
- The data have proved useful for extracting pressure-volume properties as well as making inferences about similarities of and differences between similar samples, although precisions similar to those of Z experiments¹ (1-2%) are only available if great care is exercised in alignment.

Difficulties encountered include the following:

- We had hoped to find a longer ramp time than that provided by the LP (long-pulse) machine configuration, but have not been able to do so thusfar. Calculations (K. Struve, personal communication) were frustrated by the continuously varying transmission properties of the pulse forming lines. The issue is not closed, however.
- VISAR data were of inconsistent quality due to crosstalk issues more recently solved, as well as to light amplitude issues and to “walking noise” (periodic noise introduced on some digitizers). The latter was reduced by recording timemarks on one channel per scope instead of on all four channels.
- Working out the system timing was unexpectedly difficult, but was accomplished.
- Alignment of the target hardware was more difficult than expected; to correct this will require major redesign of the Saturn MITL configuration.

3.0 Other Configurations, Validations and Diagnostics

3.1 Single-sided slab drive concept

A single shot was performed to test a new short circuit configuration that would increase the magnetic pressure through an increase in the effective current density. If successful this new configuration would be fielded on the Z accelerator in an attempt to increase the achievable flyer plate velocity for Hugoniot experiments. The concept behind this experiment was to offset the cathode in the anode box such that the AK gaps surrounding the cathode were asymmetric. The difference in inductance between the four gaps would result in an uneven current distribution on the four anode surfaces, with a larger current density on one side of the anode. This design is shown schematically in Fig. 3.1.1

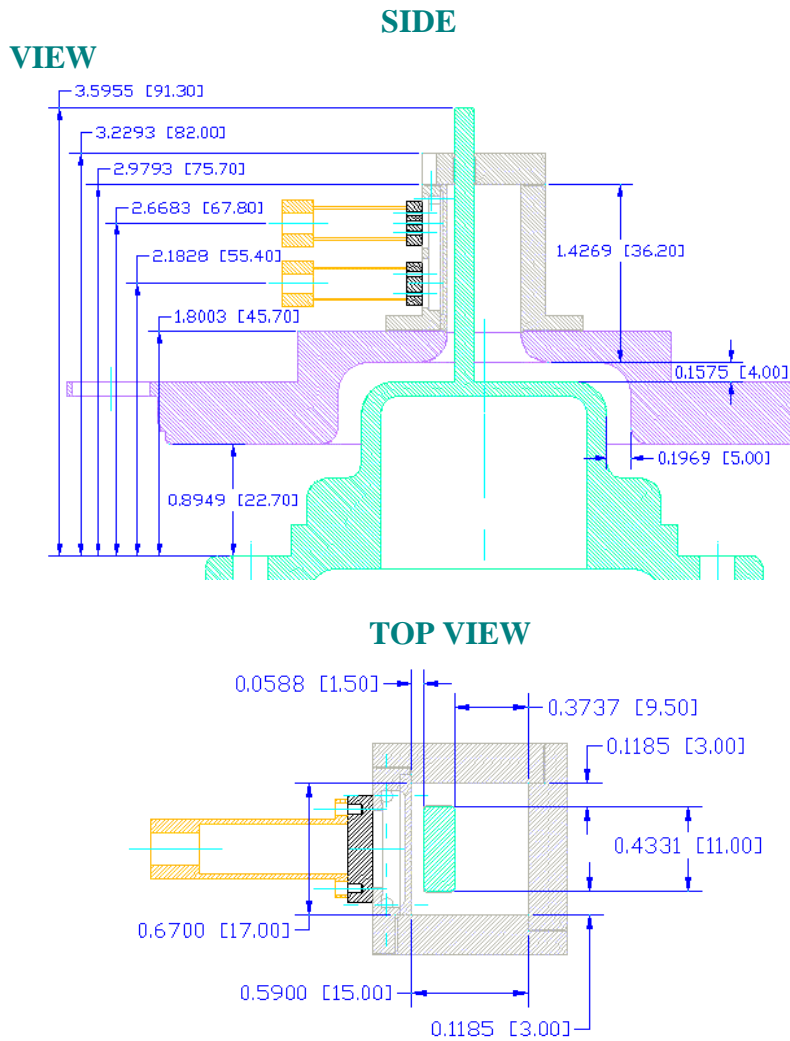


Figure 3.1.1. Configuration of single-sided slab experiment

A total of six VISAR measurements were obtained to assess the flyer plate velocity (and thus the peak magnetic pressure) as well as the uniformity of the flyer, both in the horizontal and vertical directions. The resulting VISAR records are shown in Fig. 3.1.2. Notice that good uniformity was obtained for VISAR measurements along the vertical axis of symmetry. This result indicates that a steady state current distribution was achieved near the bottom of the cathode stalk. Given the offset of the cathode in the anode box, this result was uncertain and is very promising. The horizontal measurements indicate a loss of uniformity late in time (after ~ 800 ns). This loss of uniformity is due to a magnetic pressure gradient that increases with time as the geometry of the short circuit deforms during the current pulse. This result was expected.

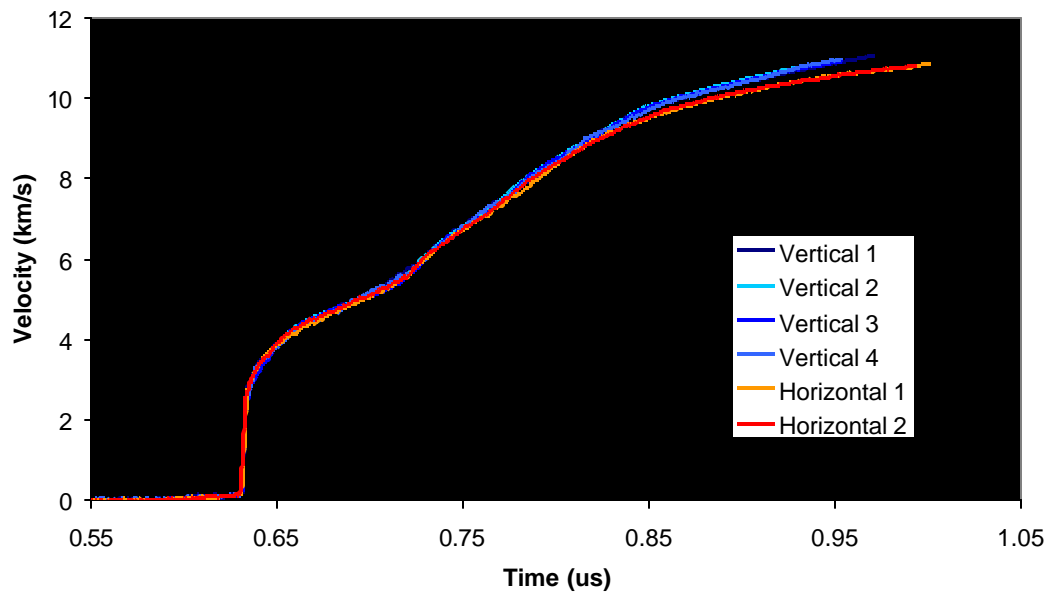


Figure 3.1.2. VISAR records from single-sided slab ICE experiment

The flyer velocity achieved in this experiment suggests that a peak magnetic pressure of approximately 750 kbar was achieved using this geometry. This is a significant enhancement in magnetic pressure relative to the two-sided slab geometry. The success of this shot is very encouraging, and has given us confidence to perform a similar experiment on the Z accelerator.

3.2 Ferroelectric and encapsulant comparison shots with containment extension

A pair of shots was performed to simultaneously assess containment options and seek differences in behavior among different compositions of the ferroelectric ceramic PZT 95/5. These materials are of interest for neutron generator design. The LP panel configuration was used atop an extension usable for mounting a sample within a containment vessel, as shown in Fig. 3.2.1. The PZT 95/5 samples were distributed so that each composition was allocated 2 panels (4 drive panels). Velocity results are shown in Fig. 3.2.2.

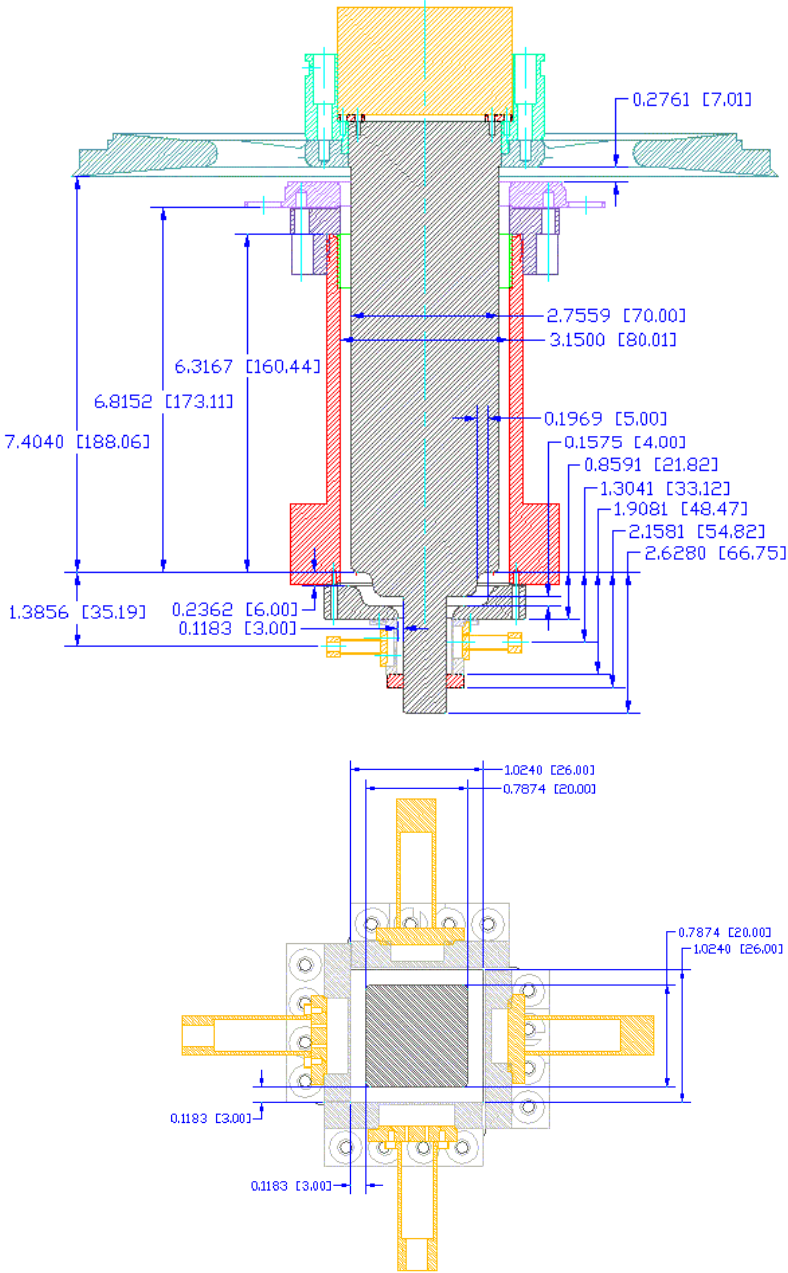


Figure 3.2.1. Configuration of PZT LP shots. Drive panels were 600 micron copper. Fused silica windows were used.

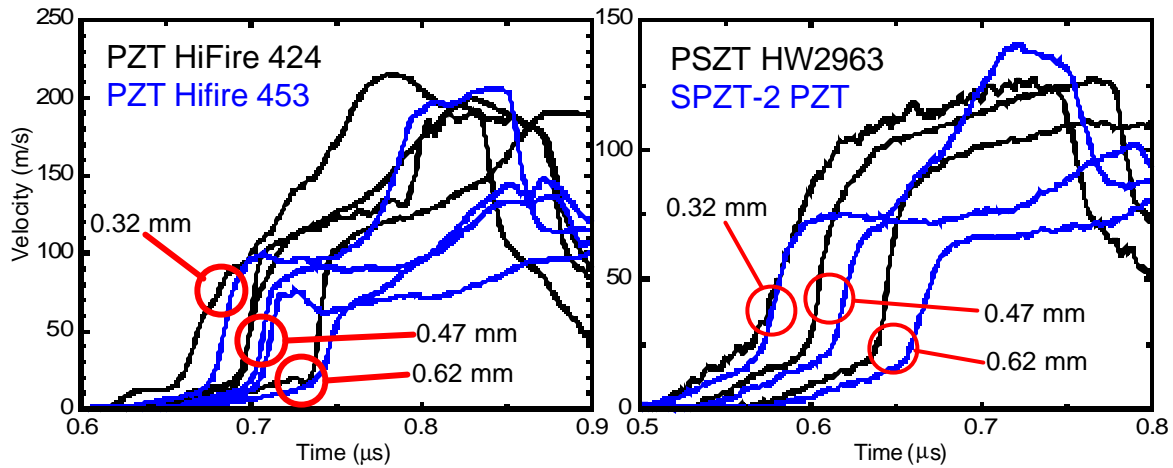


Figure 3.2.2. Velocity results from PZT tests 2912, 2919. Sample thicknesses are indicated.

Qualitatively we observe that the four types of PZT have markedly different behavior under ramp loading. The HiFire 453 and SPZT-2 samples display markedly softer behavior at the 74-100 m/s velocity level than does the Hifire 424 or PSZT HW2963 samples. This is interpreted as a pore crush zone (onset ~ 2.2 GPa). As well, the $\alpha \rightarrow \epsilon$ transition, which appears as a low ramp at the beginning of the loading, is completed at a noticeably higher velocity (and stress) for the PSZT and SPZT compositions than for the HiFire compositions.

A similar test on alumina-loaded epoxies (ALOX) with a modern hardener (459) and an older hardener (Z, which is carcinogenic) shows very little difference among the two compositions (Fig. 3.2.3). Such materials are useful as encapsulants where good high-voltage standoff is needed. Aluminum drive panels and fused silica windows were used, with Saturn in an LP mode.

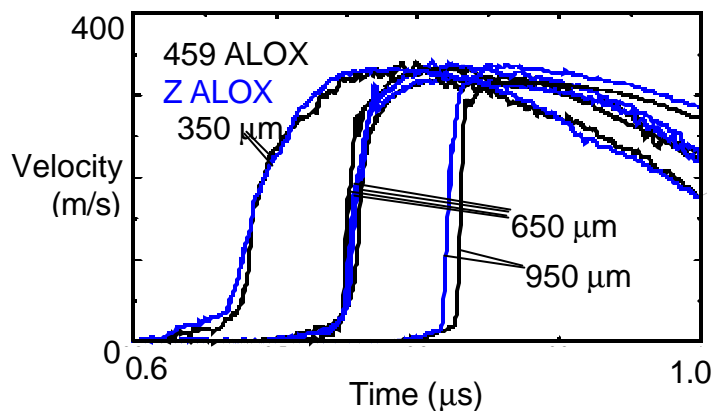


Figure 3.2.3. Velocity results from test 2913 (ALOX). Sample thicknesses are indicated.

3.3 Pre-molten tin: Resistively heated samples

Four shots on Saturn (2925-2926 and 2969-2970) were dedicated to the demonstration and development of a pre-heating technique for isentropic compression of molten tin. Dynamic freezing is a problem of interest to the Stockpile Stewardship Program, and in fact, had never been experimentally observed in metals such as tin. The ICE technique provides access to phase transitions that cannot be detected using impact experiments. The latest iteration of the heating-cell design is depicted in Fig 3.3.1. The most challenging requirement to be met is the need for a thermal insulator between the metallic drive plate (part of an enormous heat sink in the form of Saturn's power-flow hardware) and the tin sample. Materials with low thermal conductivity tend to have high elastic limits that adversely perturb the wave entering the molten tin. Pyroceram 9608, a glass ceramic made by Corning, was chosen for its ramp-generating behavior (Asay and Chhabildas, 1980).

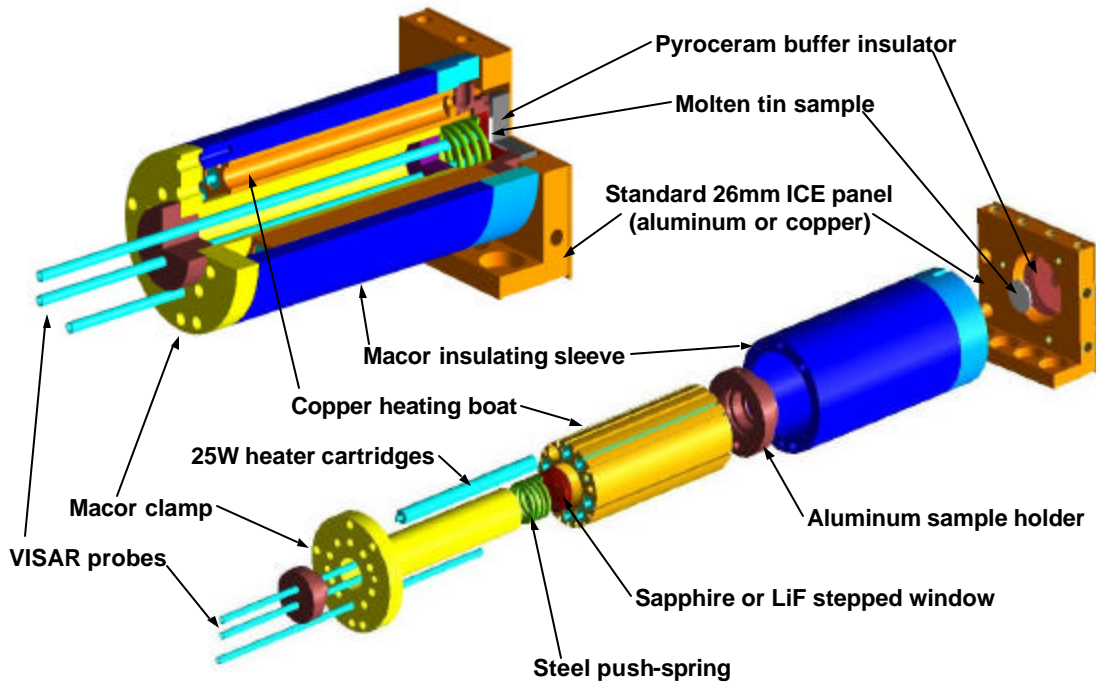


Figure 3.3.1. Resistive-heating cell used to obtain pre-molten tin samples on Saturn.

In Fig 3.3.2 are shown data from Saturn shot 2970. All of the molten tin experiments used a slab (two-sided) drive configuration with standard 26-mm anode panels, a stepped sample of molten tin on one panel, and a Pyroceram insulator without tin on the opposite panel to measure the compression wave exiting the insulator. Preliminary results suggest that dynamic freezing does occur under the present loading conditions. If further analysis of these data supports this conclusion, then Saturn will have provided important new results of high scientific and programmatic interest.

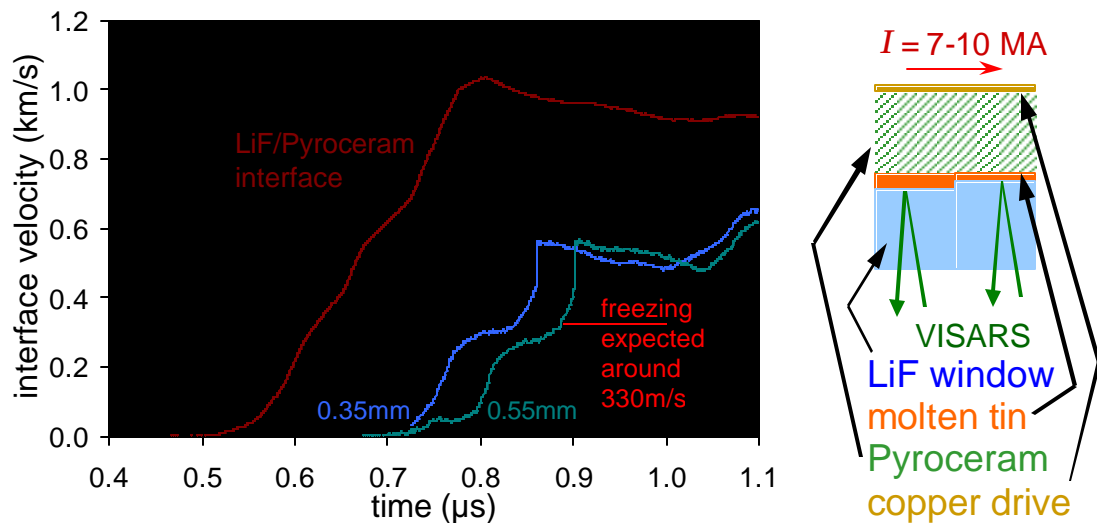


Figure 3.3.2. Example of velocity data obtained on Saturn for isentropic compression of molten tin at approximately 600K, showing a signature possibly due to dynamic freezing.

3.4 IR Pyrometry

.Experiments 2914 and 2915 used the low pressure, slab geometry. One of the two panels in each of these experiments was used for pyrometry. The pyrometer is outlined in Figure 3.4.1, left. Radiation is brought to the pyrometer by a single optical fiber. This radiation is divided in the pyrometer by dichroic beamsplitters into four spectral bands centered at these wavelengths: 1.3, 2.4, 3.5 and 5.1 microns, representing channels 1 through 4 respectively. The beamsplitters were chosen to make use of an infrared transmissive, chalcogenide (As_2S_3) glass optical fiber. The split beams are focused with coated zinc selenide lenses onto photovoltaic detectors. Channels 2 to 4 can resolve a risetime of 20 ns, channel 1 is somewhat faster. The pyrometer is calibrated while the fiber is viewing a cavity blackbody set at a sequence of temperatures. The fiber is somewhat lossy, requiring the fiber length to be short. The pyrometer was placed inside an rf isolation box set underneath the load at Saturn. Electromagnetic interference was suppressed after we had placed the digitizing scopes and a power supply inside the isolation box.

The probe viewing the experimental surface is sketched in Figure 3.4.1, right. The panel material was aluminum for experiment 2914 and copper for 2915. A VISAR probe to the side of the pyrometer fiber is not shown in the sketch; this probe was 1.5 mm above the surface. A 0.6 mm thick disk of lead (Pb) was press-fit into the counterbore. The surface of the lead was diamond turned and was not visibly deteriorated by being pressed in. The thickness was chosen so that the compression wave would shock up in the lead, bringing the lead to the melting point after the shock reached the surface. This arrangement was chosen for the simplicity of the expected signal to the pyrometer, making interpretation more likely in the presence of noise or other difficulty. The choice of thickness was based on pre-shot estimates of the current. The actual results showed a different current, giving a shock strength lower than expected. Furthermore, the desired simple output was not obtained.

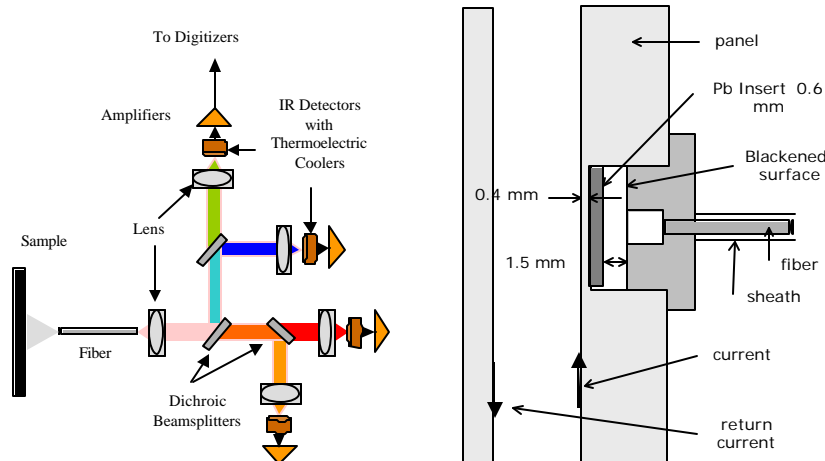


Figure 3.4.1 Left: Schematic of the Pyrometer. Right: Sketch of the Probe.

The VISAR record for experiment 2915 (copper panel) is shown at the bottom of figure 3.4.2. Experiment 2914 (aluminum panel) is qualitatively similar. The shock velocity obtained indicates that the lead surface should be at approximately 470 Kelvin (melting at 601 K). The apparent temperature recorded by the pyrometer is at the top of Fig. 3.4.2, showing far higher than 470 K. Sources of trouble were considered. For example, the possibility of fiber fluorescence due to x-rays or energetic electrons was checked on a later experiment and found to be not a problem. A tentative explanation involves the hot jet of material from the corner where the lead surface meets the counterbore. It is the nature of blackbody radiation that it increases rapidly with increasing temperature. It seems that shrouding the pyrometer's fiber was not sufficient to prevent radiation from the corner to reflect one or more times, getting into the fiber, and overwhelming radiation from the lead surface. A different experimental setup could eliminate this problem.

One part of the apparent temperature record seems to be qualitatively correct. The radiation supposed to be from a hot jet peaks at 1200 ns and then decreases. After 1500 ns a rise in temperature occurs. This is the radiation from the lead surface, now being heated by the currents induced by the penetrating B-field. The same feature was seen in experiment 2914 at an earlier time, corresponding to aluminum's lesser conductivity which allows faster B-field penetration.

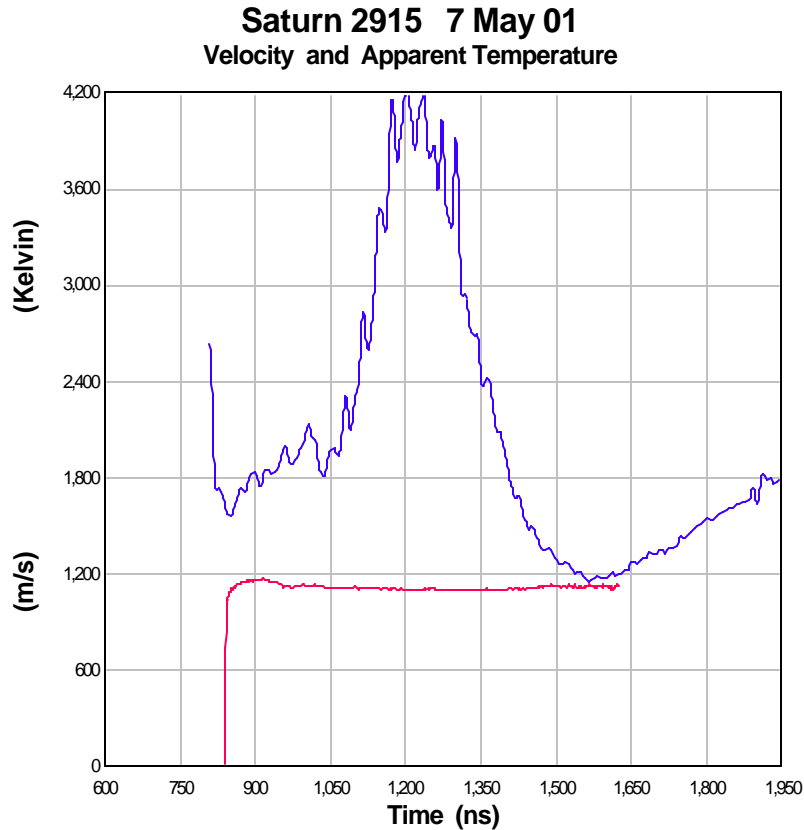


Figure 3.4.2 Bottom: VISAR Data from Saturn Experiment 2915.
Top: Apparent Temperature from the same Experiment.

3.5 Other configurations and notes

We have used ICE on Saturn for WFO; two shots for ICE on a material of interest to the Stockpile Stewardship Program, and one shot for preliminary characterization of a new low-pressure design. The latter makes use of a large square anode (60-mm panels) to reduce the peak compression to 10-20kbar for ICE studies of very low-impedance and porous materials.

As well, we have conducted a successful test to assess a concept for thermally insulating samples to allow cryogenic testing.

Careful assessments of drive uniformity within drive panels are planned for the near future as well. On shot 2968, horizontal and vertical uniformity of the drive on the low-pressure slab geometry used for the molten tin experiments was measured. This showed a peak pressure of 260kbar and good uniformity to at least 5 mm from the vertical centerline.

4.0 Overall Summary

Several difficulties have been encountered, in addition to those mentioned in Section 2.5, as follows:

1. On two shots, the current delivered to the target fell far short of that introduced into the stack. On these tests, the MITLs apparently arced, causing noticeable scars that needed to be removed by grinding. On one other configuration (the experiment with 60 mm panels), significant current was lost as well. This may have been due to electrical flow across the gap in the insert pieces (this gap was smaller than the anode/cathode gap in the test fixture).
2. Scheduling of manufacturing proved problematic. This is largely due to the need to use the same team supplying experiment hardware for the Z facility, which has become fully loaded. Protocols have been established, although the whole process involves a lead time of roughly three months at this time.

On the other hand, the greater flexibility of Saturn than of Z proved valuable in conducting a program of tests requiring learning during the course of experiments. This is evidenced by various changes successfully introduced during the course of experimentation to accommodate needs for additional VISAR spots (drive measurements, measurements of expansion of containment extensions), for additional development time for the inductive heater assemblies, and the late arrival of a batch of critical samples.

Successes mentioned earlier include:

1. The LP (long-pulse) machine configuration appears to provide a useful current structure for general-purpose ICE experiments
3. The cost is significantly below that for Z; as well, time is far more available.
4. The available pressure levels are useful
5. The data have proved useful for extracting pressure-volume properties as well as making inferences about similarities of and differences between similar samples, although precisions similar to those of Z experiments¹ (1-2%) are only available if great care is exercised in alignment..

Difficulties mentioned earlier include:

1. We had hoped to find a longer ramp time than that provided by the LP (long-pulse) machine configuration, but have not been able to do so to date. Calculations (K. Struve, personal communication) were frustrated by the continuously varying transmission properties of the pulse forming lines. The issue is not closed, however.
6. VISAR data were of inconsistent quality due to crosstalk issues more recently solved, as well as to light amplitude issues and to “walking noise” (periodic noise introduced on some digitizers). The latter was reduced by recording timemarks on one channel per scope instead of on all four channels.
7. Working out the system timing was unexpectedly difficult, but was accomplished.
8. Alignment of the target hardware was more difficult than expected; to correct this will require major redesign of the Saturn MITL configuration.

Appendix A. Additional Drawings of Experiment Hardware

Designs of the LP and HP configurations, each of which accommodate 8 samples, are shown in this Appendix. These designs include the adjacent current-flow structure.

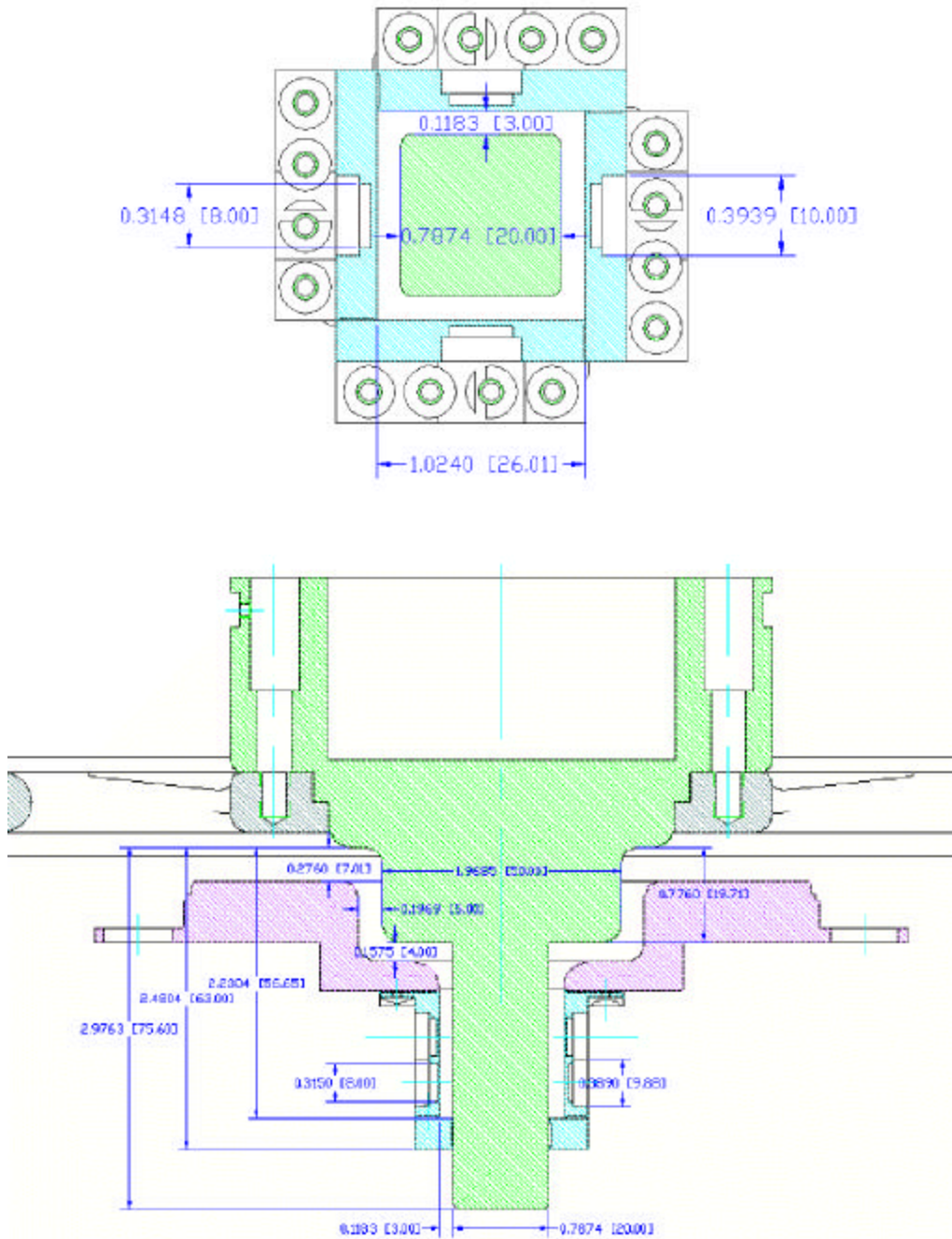


Figure A.1. LP ICE configuration. (Top) Top view (Bottom) Side view

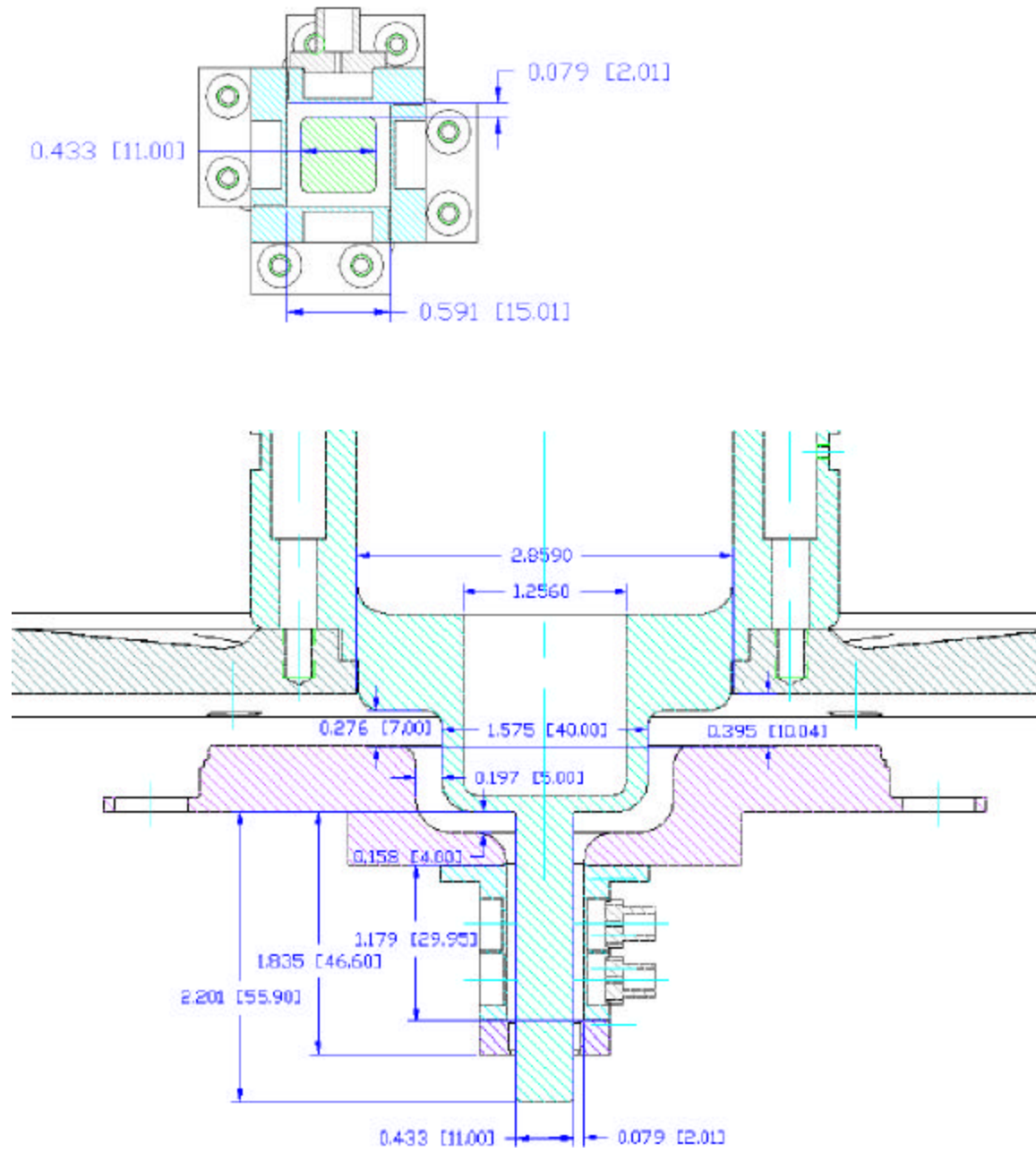


Figure A.2. HP ICE configuration. (Top) Top view (Bottom) Side view

Appendix B. Effects of various Saturn transmission line elements on pulse timing

The plots in Figure B.1 illustrate the effects of the main circuit elements on the pulse sent downline at Saturn. These pulses are chosen for each of the 36 lines, and added at the experiment to give the pulse delivered to the experiment package. However, the addition is nonlinear, and the analysis of this addition is beyond the scope of the present report.

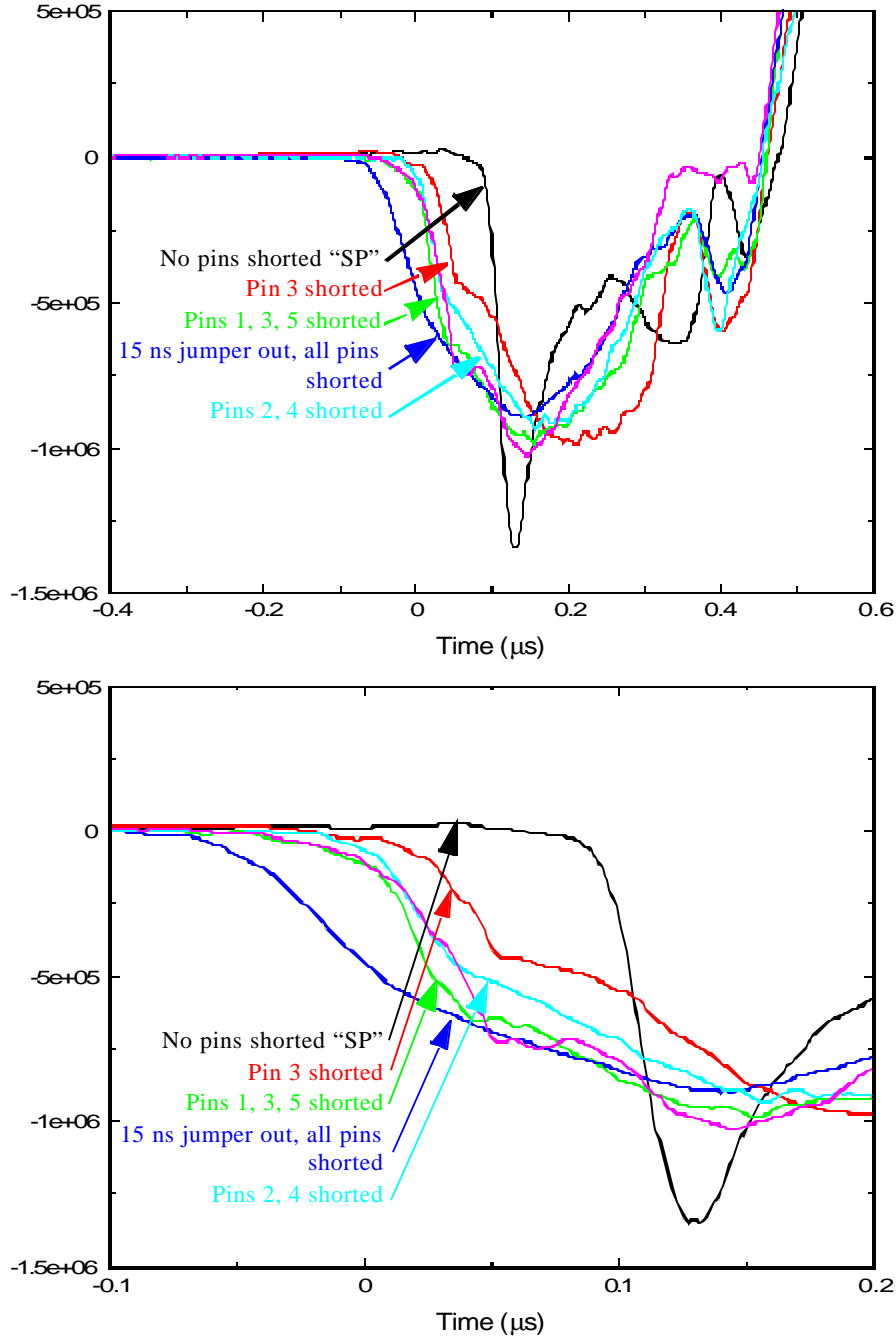


Figure B.1. Effects of circuit elements on downline pulses at Saturn (from Shot 2904)

For the “ELP” machine configuration, line configurations are set according to Table B.1. For comparison, in the LP configuration, all pins are shorted, and for the SP configuration, all are open.

Table B.1. Line configurations for Saturn shots 2904, 2906.

Line #	Jumper	Shorted Pins	Pre-Pulse Gap
1	-15	12345	Closed
2	0	3	Opened
3	0	12345	Opened
4	0	none	Closed
5	0	24	Opened
6	0	none	Closed
7	-15	12345	Closed
8	0	none	Closed
9	0	24	Opened
10	0	12345	Opened
11	0	none	Closed
12	0	135	Opened
13	-15	12345	Closed
14	0	3	Opened
15	0	none	Closed
16	0	none	Closed
17	0	24	Opened
18	0	none	Closed
19	-15	12345	Closed
20	0	none	Closed
21	0	24	Opened
22	0	12345	Opened
23	0	none	Closed
24	0	135	Opened
25	-15	12345	Closed
26	0	3	Opened
27	0	none	Closed
28	0	none	Closed
29	0	24	Opened
30	0	none	Closed
31	-15	12345	Closed
32	0	none	Closed
33	0	24	Opened
34	0	none	Closed
35	0	135	Opened
36	0	12345	Opened

For further discussion, see Section 2.3 of this report.

References

- Asay, J.R., Isentropic compression experiments on the Z accelerator, pp. 261-266 in *Shock Compression of Condensed Matter – 1999*, M. D. Furnish, L. C. Chhabildas and R. S. Hixson, eds, AIP Press, 2000.
- Asay, J. R. and Chhabildas, L. C., “Some new developments in shock wave research,” in *High Pressure Science and Technology*, eds. Vodar, B. and Mareau, Ph., Pergamon Press, 1980, pp. 958-964.
- Hall, C. A., Isentropic compression experiments on the Z accelerator, *Physics of Plasmas*, 7(5), 2069-2075, 2000.
- Hall, C. A., J. R. Asay, M. D. Knudson, W. A. Stygar, R. B. Spielman, T. D. Pointon, D. B. Reisman, A. Toor, and R. C. Cauble, Experimental configuration for isentropic compression of solids using pulsed magnetic loading, *Rev. Sci. Instr.*, 72, 3587-3595, 2001.
- Marsh, S. P. (ed.), *LASL Shock Hugoniot Data*, Univ. of California Press, 1980.
- Reisman, D. B., A. Toor, R. C. Cauble, C. A. Hall, J. R. Asay, M. D. Knudson and M. D. Furnish, Magnetically driven isentropic compression experiments on the Z accelerator, *J. Appl. Phys.*, 89, 1625-1633, 2001.

Distribution

Internal:

MS 0188	Dept. 1030	D. L. Chavez (LDRD Office)
MS 0521	Dept. 2561	S. T. Montgomery
MS 0820	Dept. 9232	P. A. Taylor
MS 1106	Dept. 15342	K. Mikkelson
MS 1106	Dept. 15342	B. Peyton
MS 1106	Dept. 15342	M. Torres
MS 1106	Dept. 15342	R. Westfall
MS 1152	Dept. 1642	M. L. Keifer
MS 1153	Dept. 15330-1	M. T. Buttram
MS 1156	Dept. 15322	R. D. M. Tachau
MS 1159	Dept. 15344	M. A. Hedemann
MS 1159	Dept. 15344	C. A. Hall
MS 1159	Dept. 15344	W. Barrett
MS 1168	Dept. 1612	D. L. Barker (BN)
MS 1168	Dept. 1612	T. Bergstresser
MS 1168	Dept. 1612	C. Deeney (10)
MS 1168	Dept. 1612	M. D. Furnish (10)
MS 1168	Dept. 1612	E. W. Marsh (BN)
MS 1168	Dept. 1612	G. A. Mize (BN)
MS 1170	Dept. 15310	R. D. Skocypec
MS 1178	Dept. 1630	D. D. Bloomquist
MS 1178	Dept. 1637	F. W. Long
MS 1179	Dept. 15340	J. R. Lee
MS 1181	Dept. 1610	J. R. Asay
MS 1181	Dept. 1610	J-P. Davis
MS 1181	Dept. 1610	M. D. Knudson
MS 1186	Dept. 1674	T. Mehlhorn
MS 1186	Dept. 1674	R. J. Lawrence
MS 1186	Dept. 1670-1	J. F. Seamen
MS 1190	Dept. 1600	J. P. Quintenz
MS 1191	Dept. 1670	K. Matzen
MS 1192	Dept. 1670-1	T. Gilliland
MS 1192	Dept. 1670-1	C. Russell
MS 1193	Dept. 1673	J. L. Porter
MS 1193	Dept. 1645	J. E. Maenchen
MS 1194	Dept. 1640	D. H. McDaniel
MS 1194	Dept. 1644	K. W. Struve
MS 9018	Dept. 8945-1	Central Technical Files
MS 0899	Dept. 9616	Technical Library (2)
MS 0612	Dept. 9612	Review and Approval Desk (For DOE/OSTI)

External:

Bechtel Nevada
Attn: S. Goldstein
MS NLV066
P. O. Box 98521
Las Vegas, NV 89193-8521

Bechtel Nevada
Attn: S. Becker
MS NLV076
P. O. Box 98521
Las Vegas, NV 89193-8521

Lawrence Livermore National Laboratory
Attn: D. Reisman
MS L-041
Box 808, Livermore, CA 94551